

**2011 NDIA GROUND VEHICLE SYSTEMS ENGINEERING AND TECHNOLOGY
SYMPOSIUM
POWER AND MOBILITY (P&M) MINI-SYMPOSIUM
AUGUST 9-11 DEARBORN, MICHIGAN**

**AUTOIGNITION CHARACTERISTICS OF LOW CETANE NUMBER JP-8
AND APPROACHES FOR IMPROVED OPERATION IN MILITARY
DIESEL ENGINES**

**Naeim Henein, PhD
Walter Bryzik, Ph.D.
Chandrasekharan Jayakumar**
Department of Mechanical
Engineering
Wayne State University
Detroit, MI

**Eric R. Sattler
Nicholas C. Johnson
Nichole K. Hubble**
U.S. Army RDECOM -
TARDEC
Warren, MI

ABSTRACT

Problems resulting from the use of low-Cetane Number (CN) JP-8 in military diesel engines are mainly caused by the poor autoignition quality of the fuel that requires a long period between the start of injection and the start of combustion. A detailed analysis of the processes which occur during the ignition delay period clearly shows that the start of combustion is preceded by a long period where the Low Temperature (LT) combustion chemistry (cool flame) prevails in which the rates of burning are very limited. Under certain operating conditions, the LT combustion regime is associated with the Negative Temperature Coefficient (NTC) regime, which adds to the length of the ignition delay period. The details of these regimes are examined by using computer simulation codes. In addition, the autoignition characteristics of JP-8 with a wide range of cetane numbers are investigated and compared with ULSD (Ultra Low Sulfur Diesel) and a Fischer-Tropsch Synthetic Paraffinic Kerosene (FT SPK) type fuel. The experimental investigations are carried out on a single-cylinder research diesel engine as well as on a heavy-duty diesel engine. The paper presents approaches for improved operation of military diesel engines on JP-8 with a wide range of cetane numbers.

INTRODUCTION

The Single Fuel Policy requires military ground vehicles to operate on JP-8 fuel. Ideally, operating vehicles on JP-8 fuel occurs without loss in maximum power and fuel economy, without any increase in black smoke at heavy loads and transient modes, and without white smoke during cold start [1, 2, 3]. JP-8 has a wide range of CNs that can be as low as 25 or higher than 74 for FT SPK type fuel [1, 4, 5]. Low CN JP-8 blends have fairly long ignition delays (ID) that if used in diesel engines without adjustments, can cause power loss, an increase in fuel consumption, unsteady operation or even complete failure of certain engine parts. Such problems are not allowable in the field because they impact survivability and mission readiness. The goal of this paper is to analyze the autoignition characteristics of JP-8 and compare it with other fuels which may be used in military vehicles. The analysis included the use of Computational Fluid Dynamics (CFD) diesel cycle simulation codes to gain more insight and a better understanding of the processes that

cause the long ID of hydrocarbon fuels and their sensitivity to different engine operating parameters. The experimental investigations are conducted on a single cylinder research diesel engine and a production heavy-duty multi-cylinder diesel engine. The two engines are equipped with common rail injection systems. Approaches to improve the operation of military diesel engines on the low CN JP-8 fuel are presented.

EXPERIMENTAL SET-UP

1. Single-cylinder research diesel engine

The engine is a PNGV (Partnership for New Generation of Vehicles), direct injection, 4-valve, water-cooled, small bore, high speed diesel engine equipped with a common rail injection system capable of delivering injection pressures up to 1350 bar. The engine simulates running under turbocharged conditions by using electrically-heated compressed shop air. The intake and exhaust pressures are also controlled to typical turbocharged diesel engine

conditions. The details of the experimental setup and procedures are given in Ref. [6, 7, 8].

2. Multi-cylinder production heavy-duty diesel engine

The commercial engine is a 4.5 L turbo charged, intercooled diesel engine equipped with a high pressure common rail injection system and a variable geometry turbocharger. The engine is equipped with an open Engine Control Unit (ECU) in addition to the production ECU. As expected, the production ECU is designed to control the engine parameters and achieve the production targets while using ULSD fuel. The open ECU allows the capability to conduct experiments under specified conditions to determine the combustion characteristics of many fuels in addition to ULSD.

3. Fuels

Table 1 gives the specifications for the low CN JP-8 and other fuels tested in this investigation.

	ULSD	JP-8 #44	FT SPK	JP-8 #31
Density (kg/m ³)	836.5	770	736.2	754.3
Cetane Number	45.3	44.1	>74	31
Flash Point (°C)	64	56.8	37.8	53
Heating Value (MJ/kg)	41.2	42.1	44.1	43.3

Table 1: Fuel Properties

4. Procedure

- Determine the combustion characteristics of JP-8#31 in the heavy-duty production engine under the OEM strategy by using the production ECU. Determine the effect of load on the combustion of JP-8#31.
- Apply a CFD simulation code to determine the effect of charge temperature on combustion regimes.
- Examine the effect of charge temperature on autoignition and combustion of JP-8#31 and other military fuels in the PNGV single-cylinder engine.
- Introduce approaches to improve the operation of military diesel engines on JP-8#31.

AUTOIGNITION AND COMBUSTION CHARACTERISTICS OF JP-8#31 IN A PRODUCTION HEAVY-DUTY ENGINE

This investigation is conducted while the engine is operating under the control of its production ECU, at a constant speed of 1800 rpm and different loads. Analysis of the data indicated that the production strategy calls for the delivery of the fuel in two events under light loads, and in one event under higher loads. The tests covered a low load of IMEP of 5 bar with two injection events and higher loads of IMEP of 10 bar, 15 bar and 18 bar with one injection event. The data reported in this paper is for the lowest and highest loads, presented for comparison.

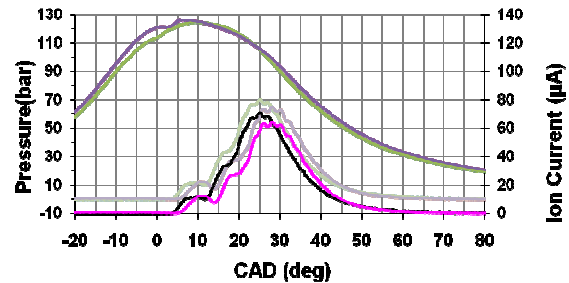
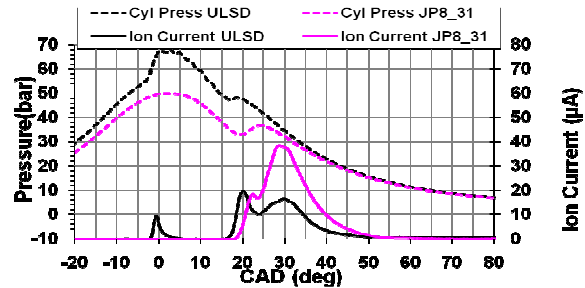


Figure 1: Cylinder Gas Pressure and Ion Current for JP-8#31 and ULSD fuels (HD Production Engine, 1800 rpm, Upper IMEP = 5 bar, Lower IMEP = 18 bar)

Figure 1 shows traces for the cylinder gas pressure and ion current produced from the combustion of JP-8#31 and ULSD fuels. Ion current signals have been found to be a good indicator of diesel combustion [11, 12]. The top figure is for an IMEP of 5 bar and the bottom figure is for an IMEP of 18 bar. At an IMEP of 5 bar, the gas pressure trace for ULSD shows a sharp rise starting at three degrees before Top Dead Center (TDC) caused by the combustion of the first injection event. Also, the pressure trace for ULSD shows another increase during the expansion stroke at 16 degrees after TDC, caused by the combustion of the second injection event. The corresponding ion current trace shows sharp increases for the two injection events. Interestingly, the pressure trace for JP-8#31 does not show any change that corresponds to the first injection. However, it does show a

clear response to the second injection event. The comparison between the traces for the two fuels indicates that the engine misfired in the first injection event due to the long ID of JP-8#31. It is noticed that the ignition delay of the combined two injection events for JP-8#31 is longer than the ID of the second injection event of ULSD fuel. The figure for IMEP of 18 bar reflects the pressure recorded in a single event fuel delivery. It is noticed that the pressure trace for JP-8#31 closely follows the trace for ULSD, with a phase shift of about 3 Crank Angle Degrees (CAD). This experiment indicates that the combustion of JP-8#31 improves at the higher load.

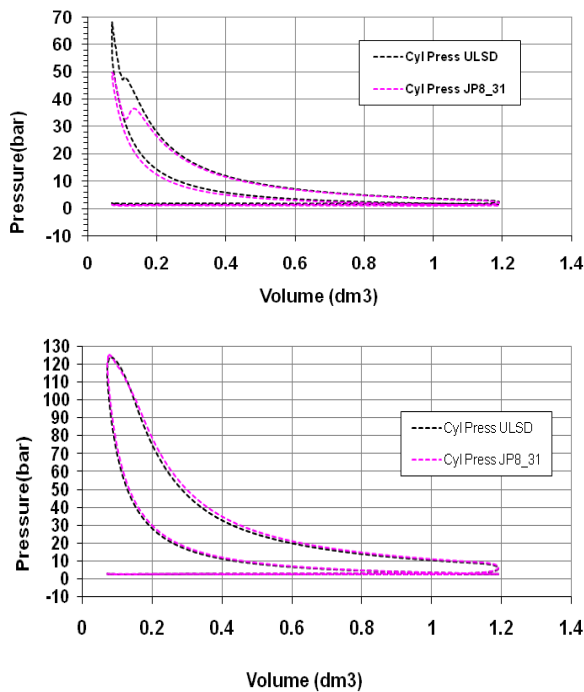


Figure 2: Comparison between the P-V diagrams for JP-8#31 and ULSD. Top IMEP = 5 bar, bottom IMEP = 18 bar. Engine speed – 1800 rpm

Figure 2 shows the Pressure-Volume (P-V) diagrams for JP-8#31 and ULSD at an IMEP of 5 bar (top) and an IMEP of 18 bar (bottom), respectively. It is clear by comparing the two figures that the combustion of JP-8#31 under higher load is improved and came closer to the combustion of ULSD.

The above analysis suggests that JP-8#31 combustion improves at the higher temperatures produced in the engine under higher loads. Based on this observation, the effect of the increase in the charge temperature on the autoignition and combustion of JP-8#31 is investigated by two

approaches. The first is by computer simulation and the second by experiments conducted on the single-cylinder PNGV engine.

SIMULATION OF THE AUTOIGNITION OF HYDROCARBON FUELS UNDER ACTUAL ENGINE CONDITIONS

1. Simulation code

This simulation is carried out to gain more insight into the processes which lead to the autoignition and combustion of hydrocarbon fuels under actual engine operating conditions. It is of interest to identify the effect of the charge temperature on processes that cause the long ID of low CN fuels such as JP-8#31, particularly the LT and the NTC regimes in diesel engines. Such insight will help in identifying approaches for improving the operation of military engines on fuels that have low CNs.

The simulation utilizes the STAR-CD CFD software package coupled with chemical kinetics mechanisms (using DARS-CFD). The combustion chamber of the PNGV engine is divided into six sectors, each containing one spray of the six spray injector. Es-ice software is used to create the sector mesh. Pro-STAR is used to set other parameters like atomization, combustion model, injection parameters and time-step resolutions. The simulation is done for the following engine operating conditions: IMEP = 3 bar, speed = 1500 rpm, intake pressure = 1.1 bar, Start of Injection (SOI) at 2.2 CAD before TDC, Exhaust Gas Recirculation (EGR) = 0 % and swirl ratio = 3.77. The software considers droplet trajectories, droplet break-up, collision and coalescence, wall interaction, wall heat transfer and droplet evaporation. The sector is defined by a cylindrical coordinate system. The sector mesh has 560,000 cells (70 x 50 x 160). The combustion mechanism is for n-heptane with 33 species and 120 reactions. The details of the simulation are given in reference [9]. The simulation covers a wide range of intake air temperatures starting from 30°C to 190°C in order to find out the reason behind the improvement in the combustion of JP-8#31, described earlier in this paper when the engine load increased from an IMEP of 5 bar to 18 bar.

The results of the simulation indicated combustion failure at intake air temperatures below 80°C, while the actual engine fired at lower intake temperatures. The disagreement between the model predictions and experimental results are caused mainly by the fact that the simulation is for n-heptane, while the engine used fuels that have different molecular structures and are heavier than n-heptane. In spite of this disagreement, the model results explain phenomena common to the combustion of paraffinic fuels which constitute most of the petroleum derived fuels.

2. Simulation of autoignition at an intake air temperature of 80 °C

Figure 3 shows in some detail the processes that occur in the combustible mixture from the start of fuel injection at 2.2 CAD before TDC to the start of the high temperature combustion regime at 5.5 CAD after TDC. The Rate of Heat Release (RHR) and charge temperature traces are shown in the lowest part of the figure, topped by traces for the mole fractions of the hydrocarbon radicals, traces for the mole fractions of H, O, OH, HO₂, HCHO and H₂O₂. The top part of the figure gives the percentages of the stable products of combustion: CO, CO₂, H₂O and O₂. The period from SOI to the sharp rise in RHR can be divided into six segments based on the major processes which affect the RHR in each segment. Particular attention is given to the processes that occur in the LT and NTC regimes that contribute in the long ID of low CN fuels.

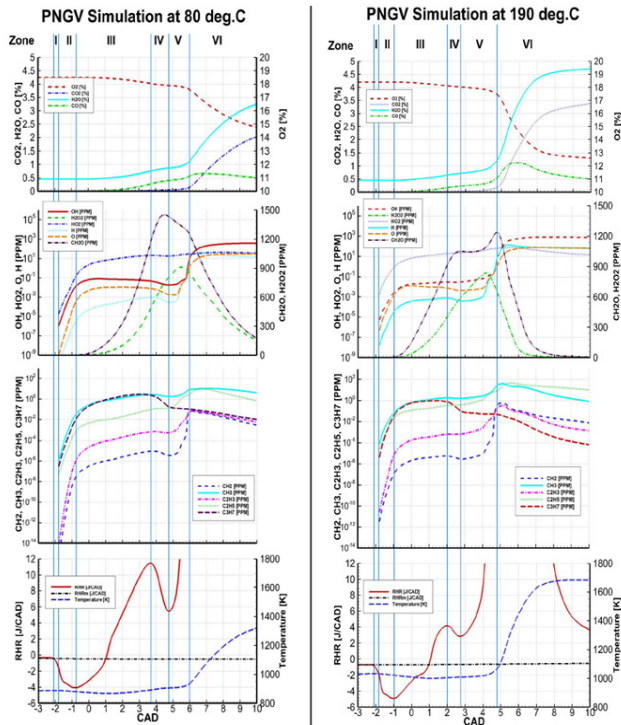


Figure 3: Simulation of RHR and species mole fractions during the ID under engine operating conditions

- I. This period is about 0.4 CAD (0.44 ms), dominated mainly by fuel evaporation. At the end of this period RHR dropped to -1.5 J/CAD.
- II. This period is 0.95 CAD (1 ms), dominated by the following processes: (a) break down of the stable fuel molecules by endothermic reactions, as evidenced by sharp increases in the mole fractions

of many hydrocarbon radicals such as CH₂, CH₃, C₃H₃, C₂H₅ and C₃H₇, (b) formation of radicals such as O, H, OH and HO₂ and H₂O₂, (c) formation of partial oxidation products such as formaldehyde (HCHO). RHR dropped at a faster rate at the beginning of this period due to endothermic reactions, followed by a slower rate due the contribution of the exothermic reactions that formed OH, HO₂, HCHO and H₂O₂. At the end of this period RHR reached a bottom value at - 4 J/CAD.

- III. This period is characterized by the following: (a) a gradual increase in hydrocarbon radicals, (b) an increase in the formation of CH₂O (HCHO), (c) an increase in H₂O₂ at a slower rate than that of HCHO, (d) a leveling off, or minor changes in mole fractions of the other species, (e) formation of stable final products such as H₂O and CO. During this period RHR increased from - 4 J/CAD to 11.5 J/CAD. Period III represents the low temperature (LT) combustion regime, referred to as cool flame.
- IV. During this period (a) most of hydrocarbon radicals dropped slightly, (b) H, O and OH dropped slightly, (c) HCHO reached its peak, (d) H₂O₂ kept increasing (e) CO and H₂O increased. RHR dropped sharply from 11.5 J/CAD to 5.5 J/CAD indicating a slowing down in the exothermic reactions. This period is referred to as the Negative Temperature Coefficient (NTC) regime where the oxidation reactions slow down, in spite of the increase in the temperature.
- V. This period is characterized by (a) an increase in the hydrocarbon radicals, (b) a sharp increase in H, O and OH (c) H₂O₂ reached its peak, (d) a partial drop in HCHO, (e) an increase in CO, H₂O and formation of CO₂. During this period RHR increased at a sharp rate indicating the start of the high temperature combustion regime.
- VI. This period represents the high temperature combustion regime where the following processes occur: (a) hydrocarbon radicals started to decrease, (b) H, O, OH and HO₂ leveled off, (c) HCHO dropped, (d) H₂O₂ dropped, (e) CO started to decrease and (f) O₂ dropped at a sharp rate indicating a high rate of oxidation as evidenced by the sharp rise in CO₂ and H₂O.

It is interesting to observe the role of HCHO in the autoignition process. It started to form in period III, after the sharp rise in the mole fractions of the following radicals, H, O, OH and HO₂. The rise in HCHO coincided with the start of the LT regime where most of the endothermic reactions slowed down or leveled off. When HCHO reached close to

its peak value, the NTC regime started indicating a drop in the rates of the oxidation reactions. When HCHO began to decrease, mostly all other species showed sharp increase. This is followed by a sharp drop in HCHO and a sharp increase in CO₂ and H₂O.

3. Effect of raising intake air temperature to 190 °C

Figure 3 shows that raising the temperature from 80°C to 190°C caused the temperature at SOI to increase from 885K to 1030K, respectively. This increase in temperature produced the following effects:

1. A larger drop in RHR in period I caused by the higher rates of evaporation due to the higher charge temperature.
2. Enhanced endothermic reactions as evidenced by the higher mole fractions of hydrocarbon radicals, H and O. This resulted in a larger drop in RHR from - 4 J/CAD to -5 J/CAD.
3. A shorter period and delta RHR for the cool flame.
4. Lower mole fractions of HCHO.
5. Higher rates of oxidation reactions that resulted in a higher rate of O₂ disappearance, and the corresponding fast rise in CO₂.

The above simulation indicated that the increase in charge temperature enhances the oxidation reactions in the low temperature combustion regime which shortens the transition period to the NTC regime. This is in addition to shortening the period of the NTC regime. If we consider the ID delay to be periods I to IV, raising the temperature from 80°C to 190°C reduced the ID from 7 CAD to 5 CAD, mostly in the LT regime. Based on this finding, some strategies were investigated in order to determine their effect in improving the combustion of JP-8#31 in military diesel engines.

COMPARISON BETWEEN THE AUTOIGNITION CHARACTERISTICS OF JP-8#31 AND OTHER MILITARY FUELS

An experimental investigation was conducted on the PNGV single-cylinder engine to compare between the autoignition characteristics of JP-8#31 and the other three fuels. Figure 4.a shows the cylinder gas pressure for all fuels at an IMEP of 3 bar and inlet temperatures of 50°C. SOI for the baseline fuel (ULSD) is adjusted to be at -2 CAD in order to keep the Location of the Peak of the Premixed Combustion (LPPC) at 5 CAD. SOI for all the fuels except JP-8#31 is kept at -2 CAD, the same as the baseline fuel. For JP-8#31 the SOI had to be advanced by four CAD for the engine to fire. The RHR for all fuels is shown in figure 4.b. It is noticed that FT SPK has the shortest ID compared to all the other fuels. This is expected

because FT SPK has the highest CN and lowest flash point. It should be noted that the fuel volatility is inversely proportional to its flash point [10]. RHR for FT SPK has a lower peak than JP-8#44 and ULSD fuels. This is mainly caused by the shorter ID which allows a shorter period of time for the fuel to evaporate and mix with the fresh air. JP-8#44 behaves in a similar way, with minor differences, as ULSD regarding the ID period and the RHR. But, major differences exist between the autoignition and combustion of JP-8#31 and the other fuels.

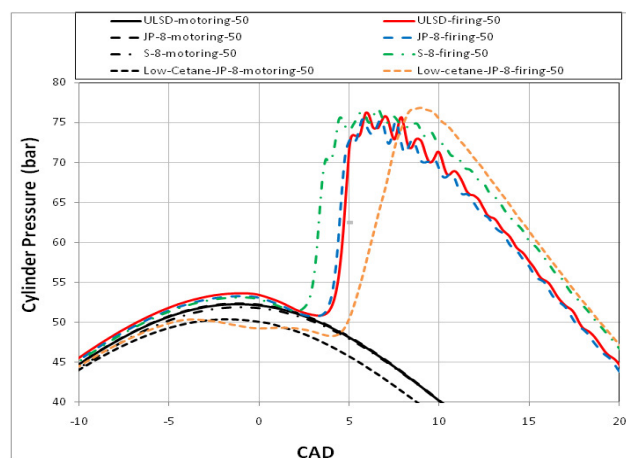


Figure 4.a: Cylinder gas pressure for different fuels at inlet air temperature of 50 °C and IMEP of 3 bar (Speed = 1500 rpm, Inj. Pressure = 800 bar, SOI = -2.0 CAD, SOI for JP-8#31 = -6.0 CAD)

Figure 4.b shows that JP-8#31 has the lowest premixed RHR peak in spite of its longest ID period which allows the longest period for evaporation. Accordingly, the lowest premixed RHR suggests that the rates of exothermic reactions of JP-8#31 are the lowest among all the fuels. The details of the autoignition process for JP-8#31 are explained in the following section.

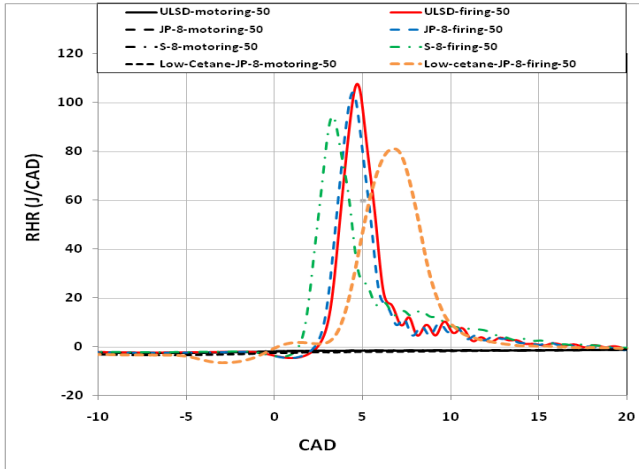


Figure 4.b: Rate of heat release for different fuels (IMEP = 3 bar, Inlet temp = 50 °C, SOI at -2 CAD except for JP-8#31 where SOI at -6 CAD)

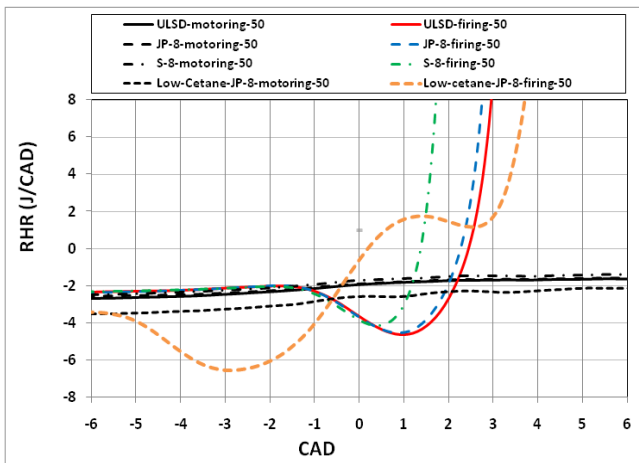


Figure 4.c: Details of RHR during the ID period of JP-8#31 and other fuels

Figure 4.c is an enlarged part of Figure 4.b that shows the details of RHR from SOI at -6 CAD for JP-8#31 and at -2 CAD for all the other fuels. The similarities between JP-8#31 trace in Fig. 4.c and the simulation traces in Figure 3 help in identifying its autoignition characteristics. Immediately after SOI, the drop in RHR is a measure of heat transferred from the air to the liquid fuel. A closer look at this part of the traces reveals that FT SPK, which has the highest volatility (lowest flash point), has the sharpest rate of drop in RHR. Also, FT SPK has the smallest dip in RHR; this is because it has the highest rates of exothermic reactions as reflected by its highest CN among all the fuels. JP-8#31 is the only fuel which showed the different combustion regimes demonstrated by the simulation. After the SOI of JP-8#31 at -6 CAD, the RHR dropped to its

lowest level after about three CADs compared two CADs for JP-8#44 and ULSD. This delay is an indication of its low rate of exothermic reactions. For JP-8#31, the low temperature combustion regime started at -2.9 CAD and continued for about 4 CAD, and raised RHR from -6.6 J/CAD to 1.8 J/CAD. The LT regime is followed by the NTC regime which lasted for about 1.2 CAD. This is followed by the high temperature combustion regime which produced high RHR. The period from SOI to the start of the high temperature combustion regime is 8.6 CAD for JP-8#31, compared to 3.2 CAD for JP-8#44.

APPROACHES TO IMPROVE ENGINE OPERATION ON JP-8#31

1. Increase charge temperature

Increasing the charge temperature at SOI is particularly important when the engine is not warmed up, such as cold starting, idling and under light loads. This can be achieved by utilizing an outside aid or by applying multiple injections. In this investigation, the charge temperature is increased by heating the intake air in the single-cylinder PNGV engine. The inlet air temperature is varied from 30°C to 110°C in steps of 10°C. The data presented in this section is for 50°C and 110°C at an IMEP of 3 bar. Figure 5 shows the charge temperature at SOI at different intake air temperatures. Increasing the inlet air temperature from 50°C to 110°C had the effect of increasing the temperature at SOI of JP-8#31 from 760K to 900K. Figure 6.a shows the RHR for all the fuels. RHR of JP-8#31 is the highest among all the fuels. This can be explained by comparing between the details of the RHR traces during the ID period given in Fig. 6.b. for 110°C and Fig. 4.c for 50°C. The main difference between the two figures is in the reduction of RHR in the LT (cool flame) regime and the dip in RHR in the NTC regime. The period of time between SOI and the start of the high temperature combustion regime decreased from 8.6 CAD to 8.2CAD, and LPPC is advanced from 7.5 CAD to 6.5 CAD. This implies an increase in the rates of the early exothermic reactions caused by the increase in the charge temperature.

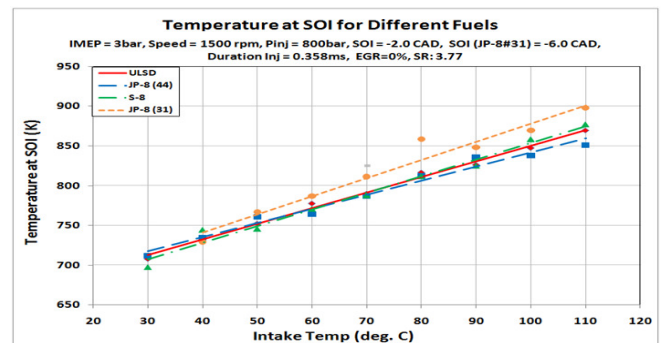


Figure 5: Effect of increasing inlet air temperature on the cylinder gas temperature at SOI (IMEP = 3 bar)

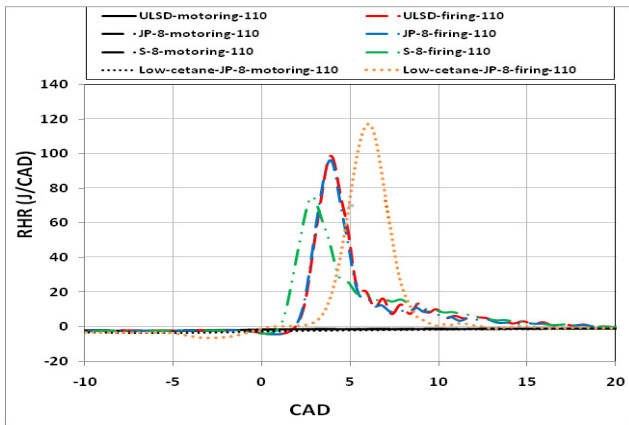


Figure 6.a: Rate of Heat Release for different fuels (PNGV engine, IMEP = 3 bar, 1500 rpm, Inlet Temp = 110 °C, SOI = -2 CAD except for JP-8#31 where SOI at -6 CAD)

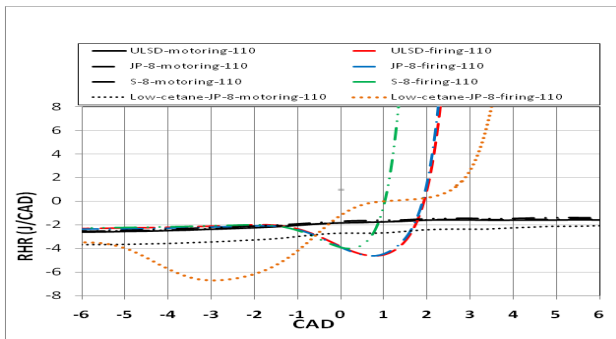


Figure 6.b: Detailed RHR, IMEP = 3 bar, Inlet Temp = 110 °C

2. Increase engine load

In this investigation, the load is increased from IMEP = 3 bar to IMEP = 5 bar while the inlet air temperature is kept at 50 °C. The increase in load allowed the engine to operate on JP-8#31 without the need to advance SOI as is the case at the lighter load IMEP of 3 bar. RHR for all the fuels is given figure 7.a and the details during the ID are given in Fig. 7.b. Comparing the RHR traces in Fig.7.b and Fig. 4.c indicates the effect of the higher load in reducing the dip in the RHR in the NTC regime.

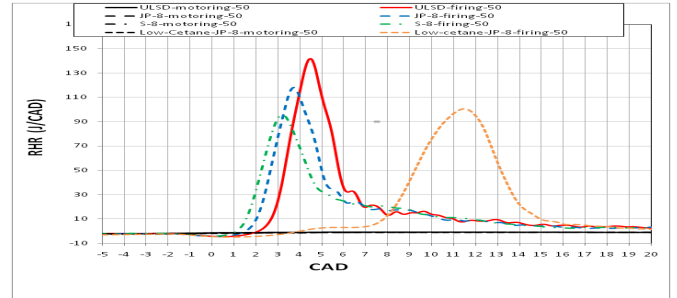


Figure 7.a: Rate of heat release for different fuels (PNGV engine, IMEP = 5 bar, 1500 rpm, inlet temp = 50 °C, SOI at -2 CAD for all fuels)

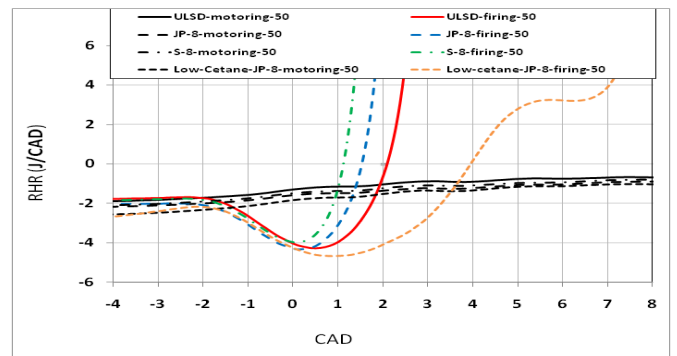


Figure 7.b: Details of the rate of heat release for different fuels during the ID period (PNGV engine, IMEP = 5 bar, 1500 rpm, Inlet Temp = 50 °C, SOI = -2 CAD for all fuels)

3. Combined increase in charge temperature and engine load

The effect of increasing the inlet air temperature from 50°C to 110°C on the charge temperature at SOI of the different fuels is given in Fig. 8.a. The details of RHR for JP-8#31 and JP-8#44 at IMEP = 5 bar and inlet air temperatures 50 and 110 C are given in fig. 8.b. It is clear that the LT and NTC regimes are eliminated by combining the increase in temperature and load.

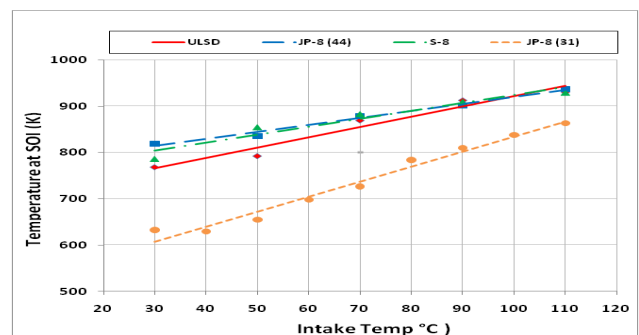


Figure 8.a: Effect of increasing inlet air temperature on the cylinder gas temperature at SOI, IMEP = 5 bar

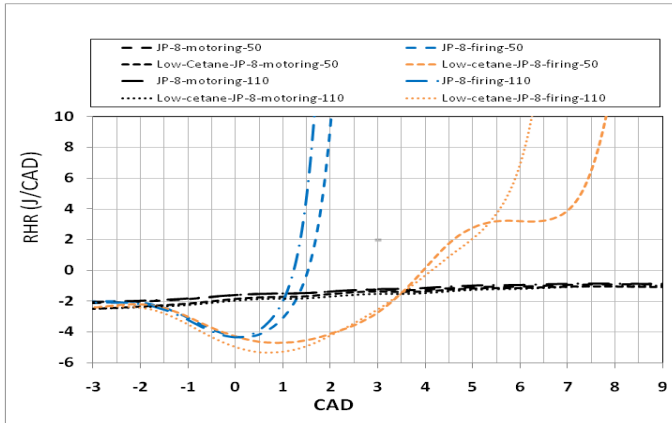


Figure 8.b: Details of the rate of heat release for JP-8331 and JP-8#44 during the ID period at IMEP = 5 bar and inlet air temps = 50 °C and 110 °C (PNGV engine, 1500 rpm, SOI = -2 CAD)

4. Effect of different approaches on fuel economy with JP-8331 and JP-8#44

		ISFC* (g/kW-hr)			
		50 °C		110 °C	
Inlet Air Temp		50 °C		110 °C	
Fuel		JP-8#31	JP-8#44	JP-8#31	JP-8#44
IMEP (bar)	3	248.73	214.36	248.23	225.35
	5	196.35	193.41	227.65	196.19

		ISFC Percentage			
		50 °C		110 °C	
Inlet Air Temp		50 °C		110 °C	
Fuel		JP-8#31	JP-8#44	JP-8#31	JP-8#44
IMEP (bar)	3	100	86.2	99.8	90.6
	5	78.9	77.8	91.5	78.9

(* - Indicated Specific Fuel Consumption)

Table 2: Effect of the increase in charge temperature and load on ISFC

The above table gives the effect of each of the proposed approaches on the indicated specific fuel consumption and its percentage of ISFC of the base line at an IMEP of 3 bar and intake air temperature of 50°C.

The table shows that the engine operation on JP-8#44 is more economical than the operation on JP-8#31. This is caused by the injection timing which is not adjusted to fit the autoignition characteristics of the low CN fuel. By proper combustion phasing the fuel economy would be the same for the two fuels.

5. Advance the SOI

In this approach, the timing of the main injection event is advanced such that combustion occurs close to TDC. This requires a combustion sensor to produce a feedback signal to the Engine Control Unit (ECU) that indicates the timing of the start of combustion or any other combustion parameter such as 10% burn or 50% burn points. Based on this input, the ECU readjusts the injection timing to achieve proper combustion phasing. The drawback of this approach is the high rates of pressure rise produced from the combustion of a large fraction of the fuel delivered during the long ID with certain fuels.

6. Advance SOI with multiple injection events to reduce Noise, Vibration, and Harshness (NVH)

To reduce the high rates of pressure produced from advancing the injection timing described above, the fuel may be delivered in two or more events. Figure 9 shows the cylinder gas pressure, needle lift (N.L) and RHR obtained on the heavy-duty diesel engine using the low ignition quality JP-8#31. The engine load is IMEP = 4 bar and speed = 1800 rpm. The data for a single injection shows a fairly high rate of pressure rise in the order of 100 bar/CAD. High rates of pressure rise produce high levels of noise and vibration and expose engine parts to excessive stresses. Using two injection events reduces the ID of the main injection and the rates of pressure rise. Figure 9 shows a pressure trace with pilot injection at 55 CAD before TDC. The rate of pressure rise is reduced from 100 bar/CAD to 20 bar/CAD and the cylinder peak pressure dropped from 70 bar to 65 bar. This caused an increase in ISFC from 187.57 g/kW-h to 196.57 g/kW-h; an increase of 4.8%. However, Brake Specific Fuel Consumption (BSFC) remained almost the same as it increased from 232.14 g/kW-h to 232.16 g/kW-h. The changes in ISFC and BSFC indicate that the mechanical losses, most of which occur around TDC, dropped with pilot injection because of the lower pressure rise rates and peak pressures reached in the cylinder. The reduction in the mechanical losses was equal to the reduction in the indicated thermal efficiency.

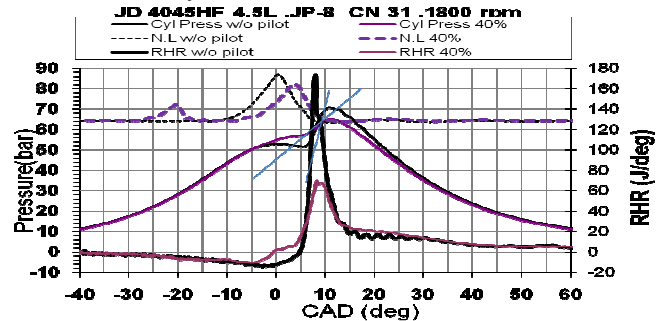


Figure 9: Traces for the cylinder gas pressure, needle lift, and RHR (HD diesel engine, JP-8#31MEP = 4 bar)

The fuel delivery strategy needs to be optimized considering the properties of the fuels most important of which for combustion are CN and volatility.

CONCLUSIONS

These conclusions are based on an experimental investigation conducted on a single-cylinder research and a heavy duty four cylinder production engine. Both engines were equipped with common rail injection systems and open ECUs. The detailed analysis of the autoignition process was done by using STAR CD and chemical kinetics mechanism for the combustion of n-heptane.

1. The autoignition and combustion characteristics of JP-8 #44 are close to the characteristics of ULSD fuel. This means that engines calibrated for ULSD fuel can operate properly, as far as combustion is concerned, on JP#44.
2. A drop of 13 units in the CN of JP-8 caused deterioration in the autoignition process of the fuel to the point of misfiring. The problem becomes much more severe if the engine is not warmed up.
3. Based on the analysis of the RHR data in the single-cylinder engine, the autoignition of the low CN JP-8 exhibited the LT combustion regime and the NTC regime.
4. The results of the detailed analysis of the autoignition processes, using CFD codes coupled with the kinetic mechanism for n-heptane showed the contribution of the different radicals in the autoignition process and the effect of the increase of the charge temperature on reducing the LT and NTC regimes.
5. Problems with low CN fuels are more serious at low charge temperatures which exist in engines operating at light loads, idling and cold start.

RECOMMENDATIONS

1. Identify the borderline CN for JP-8 for use in military diesel engines, without special aid.
2. Investigate different aids to enable military diesel engines to reliably start at low ambient temperatures on fuels of different volatilities and CN.
3. Develop the technology for the autonomous operation of military diesel engines on fuels having a wide range of properties.

ACKNOWLEDGMENT

This research was sponsored by US Army TARDEC-NAC, Automotive Research Center (ARC) sponsored by US Army TARDEC and directed by University of Michigan. The authors acknowledge the help provided by Tamer Badawy in the multi-cylinder engine experiments and Ziliang Zheng in simulated results. Special thanks are due to Laura Hoogterp from US Army TARDEC for supplying some of the fuels.

REFERENCES

1. Frame, E. A. et. al., "Alternative Fuels: Assessment of Fischer-Tropsch Fuel for Military Use in 6.5L Diesel Engine", SAE 2004-01-2961.
2. Schihl, P., et. al., "Assessment of JP-8 and DF-2 Evaporation Rate and Cetane Number Differences on a Military Diesel Engine", SAE 2006-01-1549.
3. Papagiannakis, R.G. et. al., "Single Fuel Research Program Comparative Results of the Use of JP-8 Aviation Fuel versus Diesel Fuel on a Direct Injection and Indirect Injection Diesel Engine", SAE 2006-01-1673.
4. Lepperhoff, G., et. al., "Potential of Synthetic Fuels in Future Combustion Systems for HSDI Diesel Engines", SAE 2006-01-0232.
5. Flynn, P. F., et. al., "Diesel Combustion: An Integrated View Combining Laser Diagnostics, Chemical Kinetics, and Empirical Validation", SAE 1999-01-0509.
6. Nargunde, J., Jayakumer, C., Sinha, A., Acharia, K., Bryzik, W. and Henein, N. A., "Comparison between Combustion, Performance and Emission Characteristics of JP-8 and Ultra Low Sulfur Diesel Fuel in a Single Cylinder Diesel Engine", SAE 2010 World Congress, Paper No 2010-01-1123, SP-2289, 2010.
7. Sinha, A., Jayakumar, C., Nargunde, J., Acharya, K., Bryzik, W. and Henein, N. A., "Effect of Biodiesel and its Blends on Particulate Emissions from HSDI Diesel Engine," SAE 2010 World Congress, Paper No 2010-01-0789, SP-2289, 2010.
8. Acharya, K., Dahodwala, M. Bryzik, W., Henein, N. A. and Sova, N., "The Effects of Different Biodiesel Percent Blends on Autoignition, Combustion, Performance and Engine Out Emissions from a Single Cylinder HSDI Diesel Engine", SAE 2009 World Congress, Paper No 2009-01-0489, SP- 2237, 2009.
9. Jayakumar, C., Zheng, Z., Joshi, U. M., Bryzik, W., Henein, N. A. and Sattler, E., "Effect Of Inlet Air Temperature On Auto-Ignition Of Fuels With

Different CN And Volatility”, ASME, ICEF 2011-60141, (2011).

10. Synthetic Lubricants and High Performance Functional Fluids, second edition, Leslie R. Rudnick and Reynold L. Shubkin, Marcel Dekker, Inc. New York, N.Y.
11. Henein, N. A., Bryzik, W. and Abdel-Rehim, A., “Characteristics of Ion Current Signals in Compression Ignition and Spark Ignition Engines”, SAE 2010 World Congress, Paper No 2010-01-0567, SP-2285, 2010.
12. Henein, N. A., Badawy, T., Nilesh, R. and Bryzik, W., “Ion Current, Combustion and Emission Characteristics in an Automotive Common Rail Diesel Engine”, ASME, ICEF2010-35123, 2010.

APPENDIX

A. Engine Specifications

a. Single-cylinder research diesel engine

Specification	Description
Disp. Volume	422 cm ³
Bore	79.5 mm
Stroke	85 mm
Compression Ratio	20:1
Conn. Rod Length	179 mm
Working Cycle	4-stroke diesel
Dir. Of Rotation	Counter Clockwise
Num of Cylinders	1
Rated Speed	4000 rpm (max)
Valve System	2 intake / 2 exhaust
Cooling	Ext. Water Pump
Lubrication	Ext. Oil Pump
Injection System	Common Rail
Injection Controller	ECU Controller
Intake Valve Open	353
Intake Valve Closing	-140
Exh. Valve Open	155
Exh. Valve Closing	-352
Swirl Ratio	1.44, 2.59, 3.77, 4.94, 7.12

b. Multi-cylinder heavy-duty engine

Model	4045HF485
No. of Cylinders	4 in-line
Displacement (L)	4.5
Bore and Stroke (mm)	106 x 127
Compression Ratio	17.0 : 1
Engine Type	4-stroke
Aspiration	Turbocharged
Length (mm)	860
Width (mm)	612
Height (mm)	1039
Weight (Kg)	491
Number of Valves	16

ACRONYMS AND ABBREVIATIONS

- BSFC – Brake Specific Fuel Consumption
- CAD – Crank Angle Degree
- CN – Cetane Number
- ECU – Engine Control Unit
- EVO – Exhaust Valve Opening
- FT SPK – Fischer-Tropsch Synth. Paraffinic Kerosene
- HSDI – High Speed Direct Injection
- ID – Ignition Delay
- IMEP – Inductive Mean Effective Pressure
- ISFC – Indicated Specific Fuel Consumption
- JP-8#31 – JP-8 fuel with CN=31
- JP-8#44 – JP fuel with CN=44
- LPPC – Location of the Peak of Premixed Combustion
- LT – Low Temperature
- NTC – Negative Temperature Coefficient
- RHR – Rate of Heat Release (same as ARHR)
- SOI – Start of Injection
- TDC – Top Dead Center
- ULSD – Ultra Low Sulfur Diesel